

Photoionization mass spectrometric studies of SiH_n ($n=1-4$)

J. Berkowitz, J. P. Greene, and H. Cho

Physics Division, Argonne National Laboratory, Argonne, Illinois

B. Rušćić

Physics Division, Argonne National Laboratory, Argonne, Illinois and Physical Chemistry Department, Rugjer Bošković Institute, Zagreb, Yugoslavia

(Received 8 August 1986; accepted 24 October 1986)

A photoionization mass spectrometric study of SiH_4 at $T = 150$ K reveals the presence of SiH_4^+ with an adiabatic threshold at 11.00 ± 0.02 eV. The implications for the structure of this Jahn–Teller split state are discussed. The appearance potentials of SiH_2^+ and SiH_3^+ are 11.54 ± 0.01 eV and ≤ 12.086 eV, respectively. The reaction of F atoms with SiH_4 generates SiH_3 (X^2A_1), SiH_2 (X^1A_1 and a^3B_1), and SiH ($X^2\Pi$) in sufficient abundance for photoionization studies. The measured adiabatic ionization potentials (eV) are: SiH_3 , 8.01 ± 0.02 ; SiH_2 (X^1A_1), 9.15 ± 0.02 or 9.02 ± 0.02 ; SiH_2 (a^3B_1), 8.24 ± 0.02 ; SiH , 7.91 ± 0.01 . The singlet–triplet splitting in SiH_2 is either 0.78 ± 0.03 or 0.91 ± 0.03 eV. The dissociation energy of SiH is 2.98 ± 0.03 eV. A Rydberg series is observed, converging to SiH^+ ($a^3\Pi$) at 10.21 ± 0.01 eV. Heats of formation of the various neutral and ionic species are presented, as are the stepwise bond energies of SiH_4 .

I. INTRODUCTION

In recent years, we have witnessed a flurry of activity directed at the determination of the individual heats of formation of SiH_n ($n = 1-3$), and hence the stepwise bond energies in the sequences Si, SiH , . . . , SiH_4 . Two *ab initio* calculations,^{1,2} both carried out to fourth-order Møller–Plesset perturbation theory (but one² using an empirical correction) yield similar results although differing by 4.6 kcal/mol for ΔH_f° (SiH_2). The experimental data, after some earlier wild variations have begun to settle down. A review of experimental data by Walsh,³ based largely on his own studies of the gas phase kinetics of the reaction of iodine with a series of silanes, is shown in Table I, together with the calculational results. There is general agreement regarding the heat of atomization of SiH_4 based primarily on the heat of formation of silane given by Gunn and Green.⁴ The three studies also concur (within a small uncertainty) on the strength of the first and last bonds. However, there is significant disagreement between Walsh's and the two theoretically based bond energies for the second and third bonds. In the course of the present work, Shin and Beauchamp⁵ obtained a value for the proton affinity of SiH_2 , using ion cyclotron resonance spectroscopy, and combined this with a literature

value for ΔH_f (SiH_3^+) to deduce $\Delta H_{f,298}^\circ$ (SiH_2) = 69 ± 3 kcal/mol. This value implies D_0 ($\text{H}_2\text{Si-H}$) $\cong 73$ kcal/mol, more in line with the *ab initio* results. Paralleling this upsurge of interest in the bonding properties of SiH_n , several recent studies have been directed at the ionization properties of these compounds. The HeI photoelectron spectrum has been known for some time.^{6,7} As in CH_4^+ , the SiH_4^+ parent ion is assumed to experience Jahn–Teller distortion, although heretofore not as much attention has been focused on the SiH_4^+ species by theorists as on CH_4^+ . The apparent adiabatic threshold observed by photoelectron spectroscopy is 11.6 eV.^{6,7} Three recent photoionization mass spectrometric studies⁸⁻¹⁰ yield appearance potentials for SiH_2^+ (SiH_4) ranging from 11.05 to 11.70 eV, and for SiH_3^+ (SiH_4) between 12.10–12.23 eV. Hence, unlike the situation in methane (where CH_4^+ is formed at ~ 12.6 eV and remains the only stable ion until the appearance potential of CH_3^+ is reached at ~ 14.3 eV, with CH_2^+ appearing at still higher energy¹¹), the fragment species SiH_2^+ and SiH_3^+ have an appearance potential rather near to the adiabatic threshold given by photoelectron spectroscopy. As a consequence, there has been considerable discussion in the literature regarding the stability of SiH_4^+ . One study¹³ claims to observe this species, while three others^{9,10,12} specifically say they fail to see evidence for it. A feature of the silane studies which makes this experiment a bit dodgy is the presence of the silicon isotopes of mass 29 and 30, in addition to 28, which introduces confusion between e.g., $^{30}\text{SiH}_2^+$ and $^{28}\text{SiH}_4^+$.

The HeI photoelectron spectrum of SiH_3 has been reported by Dyke *et al.*¹⁴ A long vibrational progression is observed, indicating a change of geometry from pyramidal SiH_3 to planar or nearly planar SiH_3^+ . Unfortunately, an impurity band lies in the vicinity of the adiabatic threshold, making a precise determination of this quantity somewhat dubious. In fact, a computed Franck–Condon envelope presented by Dyke *et al.*¹⁴ indicates nearly zero intensity for the

TABLE I. Recently reported bond energies in the SiH_n series (0 K).

	Pople <i>et al.</i> ^a	Ho <i>et al.</i> ^b	Walsh ^c
Si–H	69.9 kcal/mol	67.4	69.2
HSi–H	76.1	74.1	82.3
H ₂ Si–H	66.8	71.0	61.5
H ₃ Si–H	91.7	90.1	88.3
Total	304.5	302.6	301.3

^a Reference 1, as corrected in Ref. 21.

^b Reference 2.

^c Reference 3.

adiabatic process, which occurs (according to them) exactly where a prominent impurity peak appears, at 8.14 ± 0.01 eV.

No direct measurements of the ionization potentials of SiH₂ and SiH are known to us. An indirect determination of IP (SiH) can be derived from the identity

$$\text{IP}(\text{SiH}) + D_0(\text{SiH}^+) = D_0(\text{SiH}) + \text{IP}(\text{Si}). \quad (1)$$

With $\text{IP}(\text{Si}) = 8.1517$ eV,¹⁵ $D_0(\text{SiH}) \leq 3.060$ eV,¹⁶ and $D_0(\text{SiH}^+) = 3.22 \pm 0.03$ eV,¹⁷ one obtains $\text{IP}(\text{SiH}) \leq 7.99$ eV. With this background information in mind, our experimental goals were as follows:

(1) To generate as many of the free radicals SiH_{*n*} (*n* = 1, 2, 3) as possible, and to determine their ionization potentials by photoionization mass spectrometry.

(2) To determine as accurately as possible the fragmentation thresholds of SiH_{*n*}⁺ from SiH₄.

(3) To combine (1) and (2) to infer thermochemical bond energies by an alternative method than used by Walsh³ or Shin and Beauchamp.⁵

(4) To search for the elusive SiH₄⁺.

II. EXPERIMENTAL ARRANGEMENT

The basic photoionization mass spectrometric apparatus has been described previously.¹⁸ Two different target chambers were employed. For the generation of the SiH_{*n*} free radicals, a flow tube and reaction cup was employed, similar to the apparatus recently described¹⁸ for generating NH₂ by the reaction of H + N₂H₄. In this instance, F atoms were produced in a microwave discharge, and entered a cup to which SiH₄ was also introduced. The fast-flowing fluorine was removed by a cryopump.

The other target chamber, more enclosed, had a provision for the incoming gas (stable rather than transient) to be cooled to as low as 78 K. An iron-Constantan thermocouple was employed to monitor the temperature. The cooled SiH₄

was used to minimize the effects of internal energy on fragmentation thresholds, and to virtually eliminate the effect of hot bands on ionization potential measurements.

III. EXPERIMENTAL RESULTS

A. Photoionization of SiH₄

An overview of the photoionization mass spectrum of SiH₄ is given in Fig. 1. Mass 30 (²⁸SiH₂⁺) is the "prominent" ion appearing at lowest energy (~ 1075 Å), followed by mass 31 (²⁸SiH₃⁺) at ~ 1030 Å. At somewhat higher energy (~ 1000 Å $\equiv 12.4$ eV) these two species become nearly equal in intensity. Mass 28 (Si⁺) gradually appears at ~ 1025 Å and finally mass 29 (²⁸SiH⁺) becomes detectable and free of isotopic contaminants just below 900 Å. Autoionization structure appears prominently for Si⁺ and SiH⁺ at higher energy, as discussed previously by other authors.^{9,10} The photoionization mass spectrum of Fig. 1 has been "cleansed" of isotopic contaminants, i.e., the contribution to mass 31 from ²⁹SiH₂⁺ has been subtracted, leaving ²⁸SiH₃⁺.

1. SiH₄⁺

A preliminary study was performed in which the intensities of masses 30, 31, and 32 were monitored sequentially at specific wavelengths above 1000 Å. These measurements were subjected to two tests.

(a) The ratio of intensities $I(31)/I(30)$ and $I(30)/I(32)$ were plotted as a function of wavelength. If these were just isotopic variants of the same species, the ratio should be a constant, independent of wavelength. Figure 2(a) clearly reveals that $I(31)/I(30)$ has a threshold at ~ 1030 Å, and Fig. 2(b) shows that $I(30)/I(32)$ goes to the background level at ~ 1080 Å.

(b) The intensities at masses 31 and 32 were corrected for isotopic contaminants, and the residues plotted. The result for mass 32 [Fig. 2(c)] was an intensity which is weak

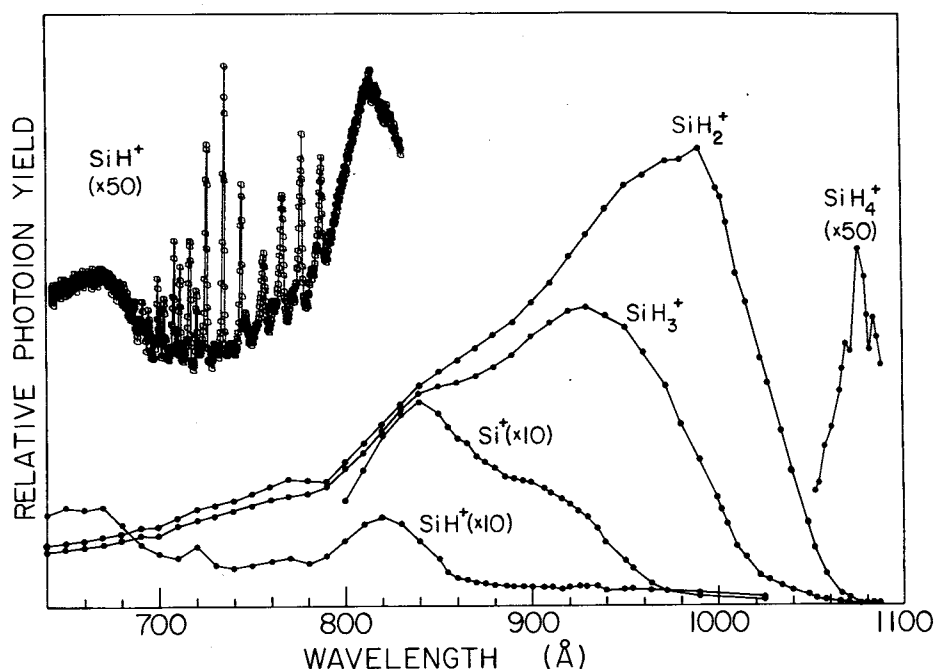


FIG. 1. Overview of the wavelength dependence (threshold to 600 Å) of the major peaks (SiH₂⁺, SiH₃⁺, Si⁺, SiH⁺) and the minor peak SiH₄⁺ in the photoionization mass spectrum of SiH₄. The relative intensities shown have been stripped of isotopic effects. The resonance structure of SiH⁺ is shown on an expanded scale. The wavelength resolution is 0.28 Å (FWHM).

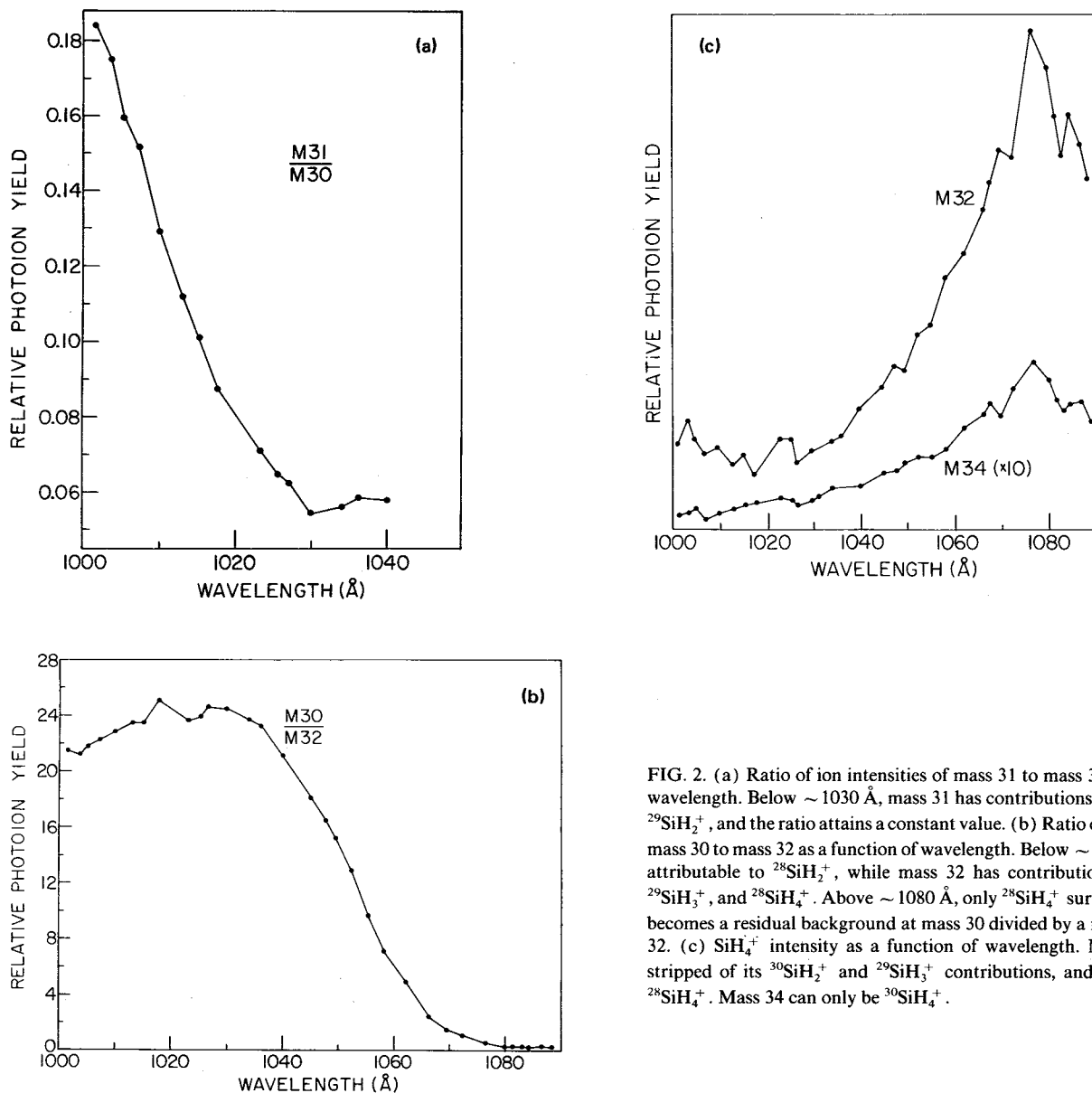


FIG. 2. (a) Ratio of ion intensities of mass 31 to mass 30 as a function of wavelength. Below ~ 1030 Å, mass 31 has contributions from $^{28}\text{SiH}_3^+$ and $^{29}\text{SiH}_2^+$, and the ratio attains a constant value. (b) Ratio of ion intensities of mass 30 to mass 32 as a function of wavelength. Below ~ 1080 Å, mass 30 is attributable to $^{28}\text{SiH}_2^+$, while mass 32 has contributions from $^{30}\text{SiH}_2^+$, $^{29}\text{SiH}_3^+$, and $^{28}\text{SiH}_4^+$. Above ~ 1080 Å, only $^{28}\text{SiH}_4^+$ survives and the ratio becomes a residual background at mass 30 divided by a real signal at mass 32. (c) SiH_4^+ intensity as a function of wavelength. Mass 32 has been stripped of its $^{30}\text{SiH}_2^+$ and $^{29}\text{SiH}_3^+$ contributions, and hence represents $^{28}\text{SiH}_4^+$. Mass 34 can only be $^{30}\text{SiH}_4^+$.

between 1000–1030 Å, then increases to a peak at ~ 1077 Å, and declines to lower energy.

This result provided convincing evidence that SiH_4^+ did exist, but that it was formed primarily at energies below the appearance of the first fragment, SiH_2^+ . To provide further verification, the weak isotopic component $^{30}\text{SiH}_4^+$ was examined at mass 34. This mass should be free of isotopic variants of SiH_2^+ and SiH_3^+ , but it is extremely weak. Nonetheless, a portion of the yield curve of this mass was obtained [Fig. 2(c)], and it mimicked the behavior of mass 32.

Thereupon, a careful study was made to determine the threshold behavior of SiH_4^+ . The experiments were performed at -150°C , which ensures that vibrational hot bands should be insignificant. The resulting data (Fig. 3) reveal step-like structure with some autoionization features e.g., at ~ 1116 Å, and a very weak onset (shown expanded) at ~ 1127 Å = 11.00 eV. Remarkably, this is about 0.6 eV below the adiabatic onset observed in the He I photoelectron

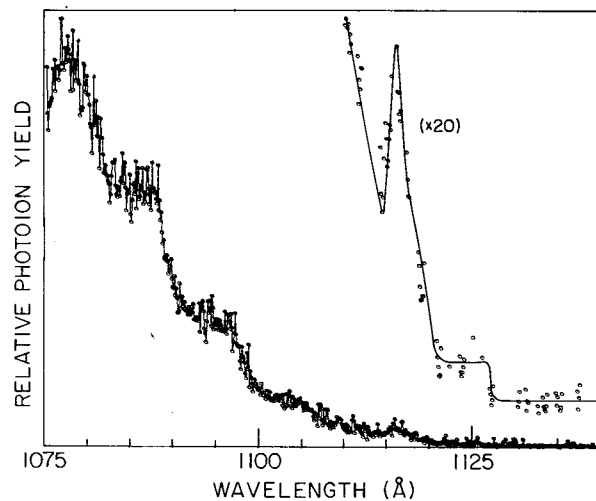


FIG. 3. The threshold region of the photoion yield curve for SiH_4^+ (M32) vs wavelength. The experiment was performed at -150°C , with a wavelength resolution of 0.28 Å (FWHM).

spectrum. However, Heinis *et al.*¹⁹ have recently measured a threshold photoelectron spectrum which "... is essentially identical with the 2T_2 bands of the He I PES. In the appearance region ... (their) TPES has a long and gradually flattening tail which merges into the background at 10.97 eV." Subsequently, these authors performed a photoionization mass spectrometric experiment¹⁰ in which "... no SiH_4^+ ions could be detected" but "the AE of the total ion current (without mass resolution) is at 11.02 eV or even lower" and the appearance energy of SiH_2^+ is 11.05 ± 0.05 eV "from the current of mass 30 which is free from isobar contributions at the AE." We agree with these authors that SiH_4 produces some ionization down to ~ 11.0 eV, but we do not agree to its attribution to SiH_2^+ .

2. SiH_2^+

The ion yield curve for mass 30 was measured in the threshold region at -150°C . The result is shown in Fig. 4. A rather distinct threshold appears at $1076 \text{ \AA} \equiv 11.52$ eV. This yield curve does not rise linearly beyond threshold, as is often observed for a fragment ion, but displays curvature. Since the total ionization is itself gradually increasing at this photon energy, presumably due to geometrical changes upon ionization (*vide infra*) and consequent Franck-Condon effects, it is not surprising to see this gradual onset. Recall that this observed threshold for SiH_2^+ is still below the adiabatic IP observed in the He I PES. When corrected²⁰ for the internal thermal energy at -150°C , the threshold for SiH_2^+ becomes 11.54 eV.

3. SiH_3^+

The ion yield curve for mass 31, after subtraction of $^{29}\text{SiH}_2^+$, is shown in Fig. 5. The subtraction was performed

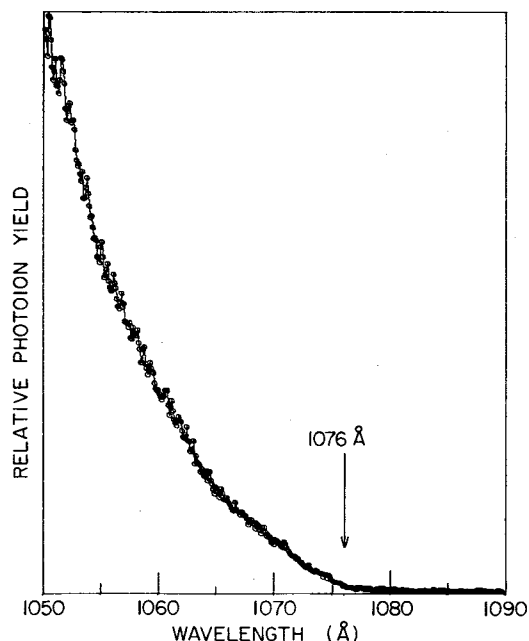


FIG. 4. The threshold region of the $^{28}\text{SiH}_2^+$ photoion yield curve from SiH_4 , obtained with the gas at -150°C and a wavelength resolution of 0.28 \AA (FWHM).

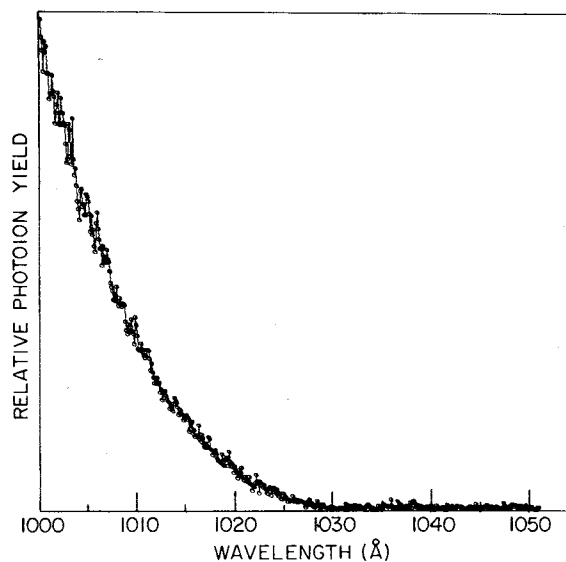


FIG. 5. The threshold region of the $^{28}\text{SiH}_3^+$ photoion yield curve from SiH_4 , obtained with the gas at -150°C and a wavelength resolution of 0.28 \AA (FWHM). A contribution due to $^{29}\text{SiH}_2^+$ has been subtracted.

digitally, by multiplying each point of the previously determined SiH_2^+ (mass 30) curve by the same factor, and reducing the mass 31 curve accordingly. The subtracted curve has a horizontal base line with a gradual, curving onset at $1027.5 \text{ \AA} \equiv 12.067$ eV. Given that this is a higher energy threshold, and that it has pronounced curvature, we shall regard this observed onset as an upper limit. (Technically, all such thresholds are upper limits, but experience has shown that linearly rising first fragment thresholds, especially within a Franck-Condon domain are accurate representations of thermochemical onsets.)

Upon correction²⁰ to 0 K, we obtain a threshold of SiH_3^+ from SiH_4 of ≤ 12.086 eV.

4. SiH^+

The ion yield curve for SiH^+ (SiH_4) has a very gradual onset (see Fig. 6). It is a much higher energy process, appearing even after Si^+ , and almost certainly suffers a delayed onset. Hence, it is not reliable as a thermochemically meaningful threshold.

5. Si^+

Although this ion is observed at lower energy than SiH^+ , its formation (either with concomitant production of 2H_2 or $\text{H}_2 + 2\text{H}$) implies a tight complex, or equivalently a small region in phase space. In this sense, it is an entropically unfavored process, and therefore is not likely to have a thermochemically significant threshold.

B. Photoionization of the free radicals SiH_n ($n=1, 2, 3$)

Fluorine atoms produced in the microwave discharge were monitored by measuring the F^+ signal at the autoionizing line (682 \AA). Silane was introduced into the reaction cup, and the F^+ signal declined. In this way, a titration could be performed, using up essentially all of the F atoms. Under these conditions, an easily measurable SiH_3^+ signal

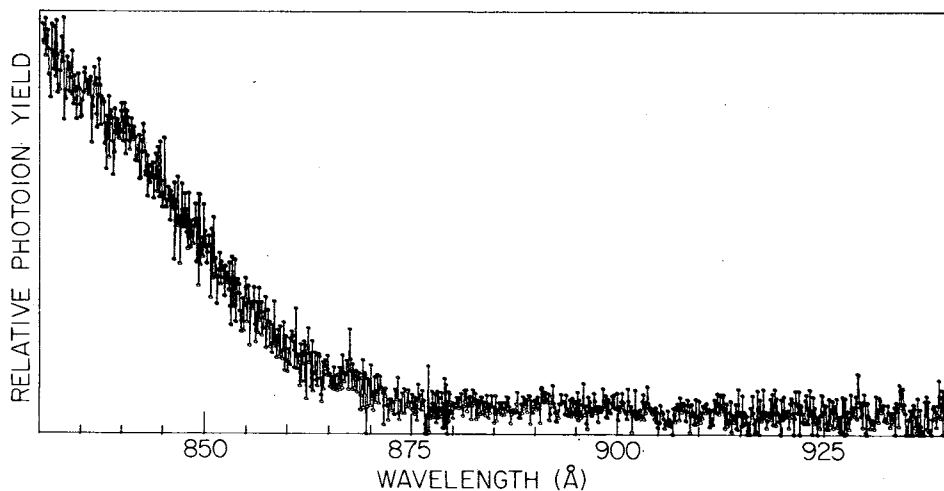


FIG. 6. The threshold region of the $^{28}\text{SiH}^+$ photoion yield curve from SiH_4 , obtained with the gas at -150°C and a wavelength resolution of 0.28 \AA (FWHM). A substantial kinetic shift is to be expected for this process, and hence the threshold is not useful for thermochemical purposes.

could be obtained at wavelengths much longer than the threshold from SiH_4 , and therefore attributable to photoionization of SiH_3 . A smaller signal of SiH_2^+ , and a still weaker one of SiH^+ could also be detected. However, for the study of SiH_2 and SiH the silane flow was reduced to maximize their respective production rates. They, of course, require successive fluorine abstraction reactions, and hence are favored by a lower SiH_4 flow rate.

1. SiH_3^+ (SiH_3)

The photoion yield curve is displayed in Fig. 7(a) from 1050 \AA to the threshold, and on an expanded scale in Fig. 7(b). The experiments were performed using only the light peaks of the hydrogen lamp. In Fig. 7(b), a step-like structure is evident from about 1390 \AA to the threshold, similar to the well-known case of NH_3 . For both cases, a pyramidal-

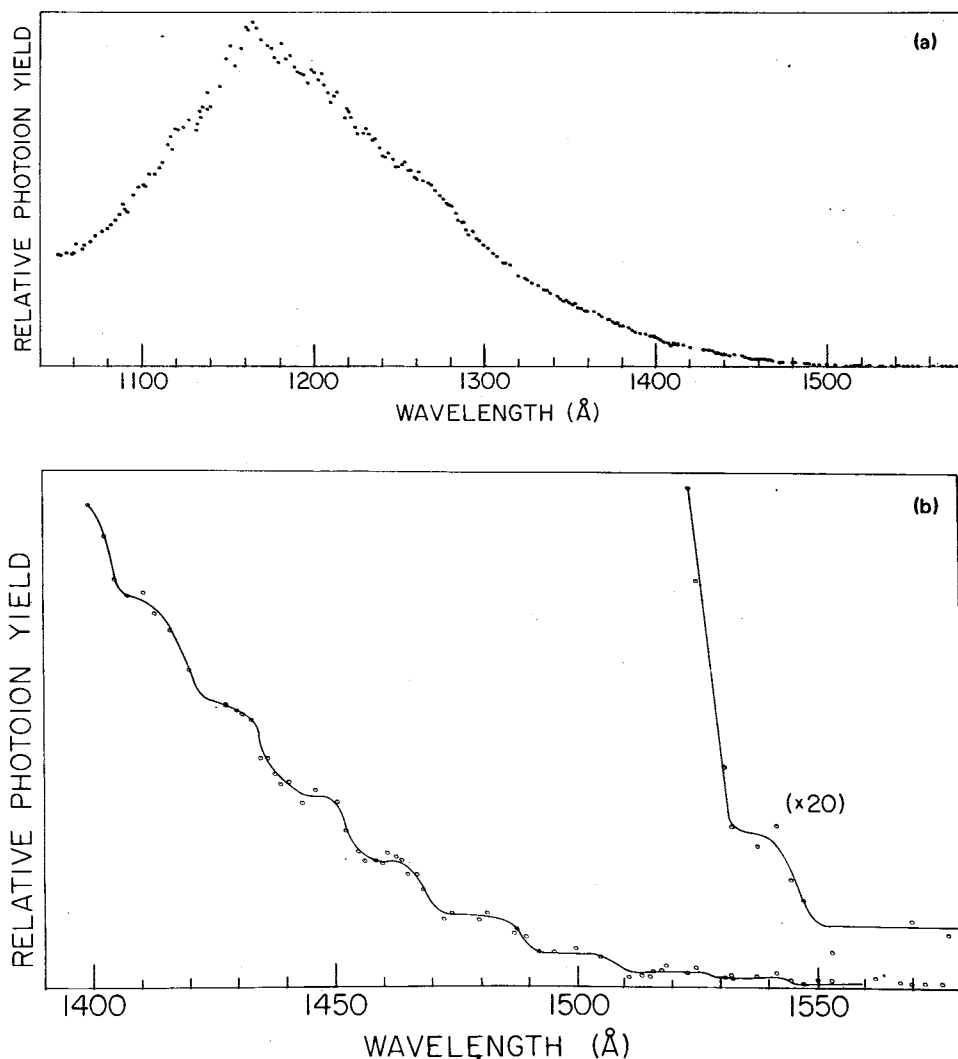


FIG. 7. (a) The photoion yield curve of SiH_3^+ from SiH_3 , from 1050 \AA to beyond the ionization threshold. (b) The photoion yield curve of SiH_3^+ (SiH_3) in the threshold region. The wavelength resolution is $\sim 0.8 \text{ \AA}$ (FWHM). The data points correspond to peak intensities in the light source.

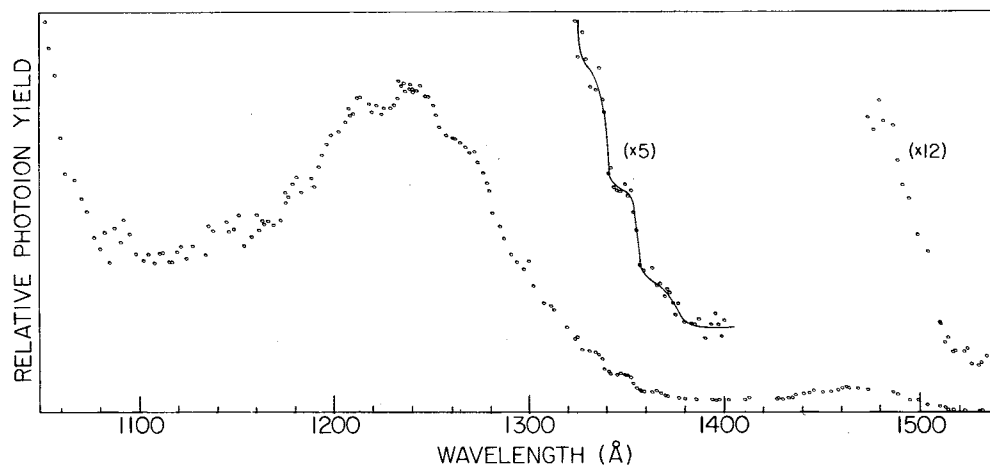


FIG. 8. The photoion yield curve of SiH_2^+ (SiH_2) from 1050 Å to beyond the ionization threshold of SiH_2 (a^3B_1). Wavelength resolution is ~ 0.8 Å (FWHM) and only the peak intensities of the light source are used. The threshold regions corresponding to SiH_2 (X^1A_1) \rightarrow SiH_2^+ (X^2A_1) and SiH_2 (a^3B_1) \rightarrow SiH_2^+ (X^2A_1) are both shown in enlarged insets.

\rightarrow planar transition is probably occurring. The step structure is indicative of direct ionization, rather than autoionization. The average step size (presumably excitation of the out-of-plane vibration) is $0.104 \text{ eV} \equiv 840 \text{ cm}^{-1}$. There is a distinct rise above the background level at $\sim 1527 \text{ Å} \equiv 8.12 \text{ eV}$. However, there appears to be an even smaller step (about 3–4 times smaller) which begins at $\sim 1547 \text{ Å} \equiv 8.01 \text{ eV}$. Five consecutive scans between a still longer wavelength (1567 Å) and the 1547 Å light peak consistently revealed some signal above background at the latter wavelength, but not at the former. Hence we take 8.01 eV as the adiabatic IP of SiH_3 .

2. SiH_2^+ (SiH_2)

The photoion yield curve of SiH_2^+ (SiH_2) was obtained in a point-by-point scan, only at the wavelengths corresponding to peak light intensities in the many-lined molecular emission spectrum of H_2 . The resulting spectrum is shown in Fig. 8. There is some hint of structure superimposed upon an approximately linearly declining curve

between ~ 1276 – 1350 Å. Some signal was observed to persist to longer wavelengths, and finally reached the background and level at ~ 1520 Å. This signal is dependent on light intensity, on F atoms and on SiH_4 . Such a signal was not observed below “threshold” for SiH_3 (above) or SiH (below). We attribute this weak signal to metastable, triplet SiH_2 , a portion of which survives collisions to reach the ionization zone. This “metastable signal” leads to some uncertainty in the selection of the adiabatic threshold for the neutral ground state, since the shape of the ion yield curve of the excited state at ~ 1355 – 1390 Å can influence our choice. There is a flat portion between ~ 1375 – 1435 Å. If we regard this as our “elevated background,” there is a noticeable increase at $\sim 1370 \text{ Å} \equiv \sim 9.05 \text{ eV}$ which could be the adiabatic IP (SiH_2). At 1355 Å there occurs a more definite increase. Therefore, $\text{IP}(\text{SiH}_2) \leq 9.15 \text{ eV}$, and could be in the neighborhood of 9.05 eV. This threshold region, as well as the lower threshold region at ~ 1520 Å are shown in enlarged insets in Fig. 8. The adiabatic IP of the metastable triplet state is chosen to be $1504 \pm 5 \text{ Å} \equiv 8.24_4 \pm 0.02_5 \text{ eV}$.

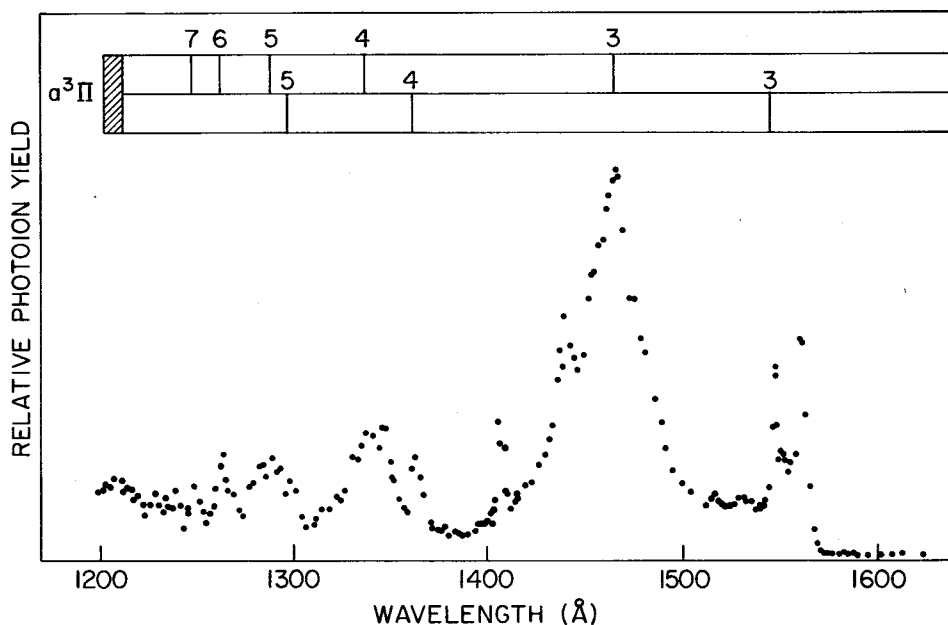


FIG. 9. The photoion yield curve of SiH^+ (SiH), from 1240 Å to beyond the ionization threshold. Wavelength resolution is ~ 0.8 Å (FWHM) and only the peak intensities of the light source are used. The Rydberg series converging to SiH^+ ($a^3\Pi$) is identified.

3. SiH⁺ (SiH)

Initially, we were hoping to see SiH⁺ as a fragment from the rather abundantly produced SiH₃, but a scan revealed some autoionizing features at the mass 29 position, which were best interpreted as due to primary ionization of an SiH species. In order to optimize this signal, it was necessary to severely limit the SiH₄ flow. Under these conditions, there was also an increase in ion background emanating directly from the microwave discharge (i.e., independent of light intensity, but sensitive to mass tuning). A compromise condition was adopted, and the photoion yield curve shown in Fig. 9 was obtained. Again, only the wavelengths of the light peaks produced by the hydrogen lamp were used in these measurements. The spectrum of Fig. 9 reveals significant autoionization structure. There is a sharp peak at ~1560 Å, near the onset. Clearly, the adiabatic ionization potential of SiH must be to longer wavelength than the peak at 1560 Å ≡ 7.948 eV. A well-defined onset occurs at 1570 Å ≡ 7.897 eV.

4. SiH⁺ (SiH₃)

By slightly increasing the flow of SiH₄ into the reaction chamber, it was possible to substantially reduce the SiH production [and hence SiH⁺ (SiH)] while optimizing the SiH₃ generation. Under these circumstances, we again examined the mass 29 ion yield curve, and obtained the spectrum shown in Fig. 10. A weak threshold is observed at 1280 ± 5 Å ≡ 9.68₆ ± 0.04 eV, corresponding to SiH₃ + *hν* → SiH⁺ + H₂.

IV. INTERPRETATION OF RESULTS

A. Ionization thresholds from SiH₄

1. SiH₄⁺

Prior to the present work, the only convincing evidence that SiH₄⁺ was sufficiently stable to be detected mass spectrometrically was that reported by Genuit *et al.*¹³ These

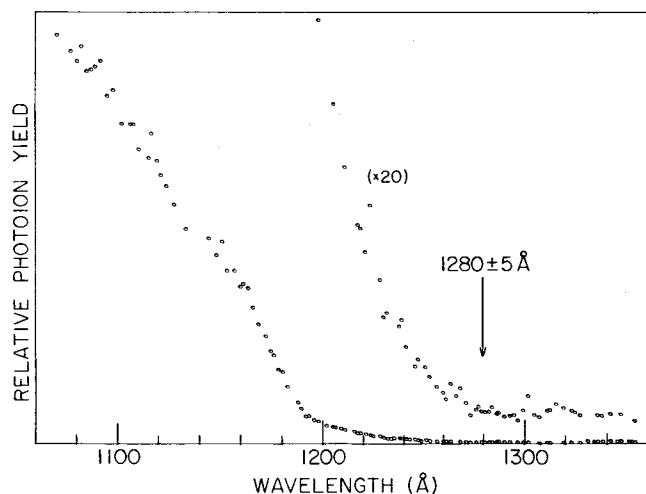


FIG. 10. The photoion yield curve of SiH⁺ from SiH₃, from 1070 to 1350 Å. The region near threshold is expanded in the inset. Wavelength resolution is ~0.8 Å (FWHM) and only peak intensities in the light source are used.

authors used the light from an Ar resonance lamp, which primarily produced 1066 and 1048 Å photons, to irradiate SiH₄. They concluded that a portion of mass 32 (after subtracting contributions from ³⁰SiH₂⁺ and ²⁹SiH₃⁺) and all of mass 34 were attributable to SiH₄⁺. They estimated that SiH₄⁺ accounted for 3%–4% of the ionization at these wavelengths. We do not know the relative strengths of the two Ar lines in their lamp, but their estimate is compatible with our observations, particularly if most of their radiation was at 1048 Å. At 1066 Å, SiH₄⁺ amounts to about 30% of SiH₂⁺.

Genuit *et al.* point out why earlier electron impact studies may have failed to observe SiH₄⁺. The thermal energy of SiH₄ in the hotter electron impact ion source, plus the width of the electron energy distribution, could cause dissociation of at least some of the SiH₄⁺. The poorer energy resolution in electron impact studies, together with characteristically weak cross sections at threshold and the isotope contamination problem combine to make detection extremely difficult.

The failure of the previous photoionization mass spectrometric studies to observe SiH₄⁺ requires some other explanation. Ding *et al.*⁹ apparently made their most careful search at 800 Å, perhaps because their monochromatized light was most intense near this wavelength. However, as we have seen in Fig. 2(c), the SiH₄⁺ ion yield curve declines from a maximum at ~1076 Å to a vanishingly small level at 1000 Å, and hence would be undetectable at 800 Å. Börlein *et al.*¹⁰ did observe total ionization down to 11.02 eV, but somehow in their experiment this correlated with a tail of the SiH₂⁺ ion yield curve, whereas “No SiH₄⁺ parent ions could be detected.” A possible explanation is that some collisional processes were occurring between the time of formation of SiH₄⁺ and its entry into the mass analyzer, such that the SiH₄⁺ was converted almost entirely to SiH₂⁺.

The SiH₄⁺ photoion yield curve [Fig. 2(c)] has distinct evidence of step structure, with half-rise points at ~1127, 1118.5, 1109, 1098.5, 1089, and 1081 Å. The average step size is 0.094 eV. The first observable peak in the *photoelectron spectrum*⁶ is at ~11.67 eV, with succeeding peaks exhibiting a spacing of 0.093 eV. The two series (PIMS and PES) appear to match, not only in their vibrational spacing, but they also appear to merge into one another at ~11.57 eV. It seems fair to conclude that it is the same vibrational mode of the ion that is excited.

The potential surface of the electronic ground state of SiH₄⁺ must be rather complicated. Pople and Curtiss²¹ have recently calculated this Jahn–Teller distorted surface, and find a saddle point with C_{2v} symmetry at about 11.47 eV, which slides down into a C_s symmetry which has a true minimum at 11.12 eV (cf. our experimental value of 11.00 eV). This most stable structure can be described as SiH₂⁺·H₂ with the SiH₂⁺ portion having shorter Si–H bond lengths (1.46 Å) and an H–Si–H angle of 120°, while the Si·H₂ moiety defines a plane perpendicular to the SiH₂⁺ plane, with longer Si–H bond lengths (~1.95 Å) and a very acute H–Si–H bond angle of 22°.

It appears as if the Franck–Condon overlap between tetrahedral SiH₄ and the aforementioned C_s symmetry of SiH₄⁺ must be very weak, essentially undetected in the photoelectron spectrum, whereas the overlap to the more sym-

metric C_{2v} , and perhaps other components of the Jahn–Teller split surface, occurs at higher energy and accounts for the bulk of the intensity in the photoelectron band.

However, the *shape* of the ion yield curve of Fig. 2(c) requires an additional explanation. The step structure near threshold suggests direct ionization. If this behavior persists to somewhat higher photon energy, then the states of the molecular ion which survive as SiH₄⁺ should continue to be made with the same efficiency. However, the SiH₄⁺ ion yield curve drops precipitously below ~ 1076 Å, and becomes negligible at ~ 1000 Å. Morrison and Traeger¹² have suggested that a predissociation process, longer-lived than direct dissociation, accounts for the onset region for formation of SiH₂⁺, based on the observation of discrete vibrational structure in the photoelectron spectrum of SiH₄. Gordon²² comes to a similar conclusion, based on the potential energy surfaces resulting from SiH₄⁺ in C_{2v} symmetry. The present observation of a precipitous decline in the SiH₄⁺ yield at higher photon energy may be further evidence of such a process.

2. SiH₃⁺

We have already pointed out that the pronounced curvature in the threshold region (Fig. 5) makes this onset a questionable one for thermochemical purposes. Nevertheless, a glance at Table II shows that four different photoionization studies, including the present one, arrive at very nearly the same threshold value. Furthermore, as Shin and Beauchamp⁵ have shown, if one combines an accepted value for $\Delta H_{f,298}^\circ$ (SiH₃) with the adiabatic IP (SiH₃) = 8.14 eV reported by Dyke *et al.*,¹⁴ one obtains $\Delta H_{f,298}^\circ$ (SiH₃⁺) = 234.1 kcal/mol, which is in very good agreement with $\Delta H_{f,298}^\circ$ (SiH₃⁺) = 235.1 kcal/mol based on the SiH₃⁺ (SiH₄) threshold.

Why, then, continue to question this threshold? We believe that the adiabatic ionization potential of SiH₃ obtained in the present work, uncontaminated by impurities, is more reliable than the value of Dyke *et al.*¹⁴ If the presently determined value is chosen, then $\Delta H_{f,298}^\circ$ (SiH₃⁺) becomes 231 kcal/mol. In order to make the SiH₃⁺ (SiH₄) threshold yield the same value of ΔH_f (SiH₃⁺), the threshold must occur at ~ 11.98 eV = 1035 Å, about 8 Å longer than observed. Alternatively, combining the appearance potential of SiH₃⁺ (SiH₄) with our IP (SiH₃) yields a bond energy

H₃Si–H of ~ 94 kcal/mol, which is 3 kcal/mol larger than obtained by various theoretical and experimental methods.^{1–3}

It should be noted that an earlier review²³ selected $D(\text{H}_3\text{Si–H}) = 96.0$ kcal/mol at 298 K (equivalent to 94.3 kcal/mol at 0 K), which would be in good agreement with the combined appearance and ionization potentials obtained in the present work. However, it was based on data reported in the 1960's, and a "low value, 89 ± 4 kcal/mol" was rejected in their evaluation. Hence, although we cannot categorically eliminate the possibility of a 94 kcal/mol bond energy, the prevailing evidence based on more recent measurements and calculations, together with the pronounced curvature in our SiH₃⁺ (SiH₄) ion yield curve appears to favor a lower bond energy.

3. SiH₂⁺

The SiH₂⁺ (SiH₄) threshold, which is the lowest energy fragmentation process, should be the most reliable. In addition, isotopic contamination from ²⁹SiH⁺ and ³⁰Si⁺ is absent, since these thresholds occur at higher energy. Despite these favorable factors, some curvature exists in the threshold curve of Fig. 4. We have minimized the contribution of thermal energy to this curvature by operating at -150 °C. Our resulting threshold, corrected to 0 K, is lower than the values of Ding *et al.*⁹ and of Corderman and Beauchamp,⁸ suggesting to us that these authors extrapolated to threshold from data at higher photon energy. The very low value for this threshold reported by Börlin *et al.*¹⁰ is difficult to explain by other than the mechanism of collisional dissociation of SiH₄⁺ mentioned earlier.

The appearance potentials of the SiH_n⁺ species obtained from SiH₄ are summarized in Table II, as are the results of the other recent photoionization studies.

B. Ionization of the free radicals

1. SiH₃

In the full scan of Fig. 7(a), the photoion yield curve of SiH₃⁺ rises to a maximum at ~ 1164 Å = 10.65 eV, and drops off rather sharply to higher energies. In the PES of SiH₃ reported by Dyke *et al.*,¹⁴ the peak of the Franck–Condon distribution of the first electronic band (the only one reported) occurs at ~ 8.8 eV ≈ 1409 Å. In Fig. 7(a), the

TABLE II. Appearance potentials of SiH_n⁺ species by photoionization (eV).

	Present data (0 K)	Börlin <i>et al.</i> ^a	Ding <i>et al.</i> ^b	Corderman and Beauchamp ^c
SiH ₄ ⁺	11.00 ± 0.02
SiH ₃ ⁺	≤ 12.086	12.10 ± 0.05	12.23 ± 0.02	12.10 ± 0.05
SiH ₂ ⁺	11.54 ± 0.01	11.05 ± 0.05	11.67 ± 0.04	11.70 ± 0.07
SiH ⁺	d	13.8 ± 0.4		
Si ⁺	d	12.65 ± 0.10		

^a Reference 10.

^b Reference 9.

^c Reference 8.

^d Delayed onset, invalid for thermochemical threshold determination.

relative photoion cross section at 1409 Å is less than 1/10 the value at 1164 Å. The large increase in ion yield between 1409 and 1164 Å is most likely related to the proximity of the first excited state of SiH₃⁺. A detailed interpretation is difficult to provide at this time. One possibility is that the very broad structure peaking at 1164 Å represents an early autoionizing Rydberg state converging to the first excited state. Its breadth implies an extended Franck–Condon region, and hence a substantial change in geometry from neutral, ground state SiH₃. The sharp decline in cross section below 1164 Å is characteristic of autoionization, rather than direct ionization.

Dyke *et al.* have reported ΔSCF vertical ionization potentials for the excited states, as well as the ground state. The first excited ionic state is calculated to be ³E, at 12.60 eV, resulting from a (2e)⁻¹ process. The electron has been removed from an Si–H bonding orbital, and hence an increase in the Si–H internuclear distance may be expected. Their ΔSCF calculation gives fairly good agreement with experiment for the first vertical IP (8.48 eV calculated vs 8.47 eV observed). If we use their 12.60 eV for the vertical second IP, and our 10.65 eV broad peak as the first autoionizing Rydberg member converging to that level, we obtain *n** = 2.64 from the Rydberg formula. This is a plausible value for the first Rydberg member; the quantum defect of 0.36 (mod 1) is indicative of substantial *p* character in the Rydberg state.

The wavelength region between 1390 Å and the ionization threshold [Fig. 7(b)] displays clear evidence of step structure, reminiscent of the NH₃ photoionization (see, for example, Ref. 11, pp. 128–130). In that case, and very likely the present one, the Rydberg states converging to the first IP are predominantly predissociated, leaving a residual weak autoionization structure superimposed upon a step structure characteristic of direct ionization. The average step width between 1435 Å and the ionization threshold is 840 cm⁻¹. This can be compared with $\bar{\omega}_e = 820 \pm 40$ cm⁻¹ obtained by Dyke *et al.* from an analysis of 14 vibrational components in their photoelectron spectrum. The calculated out-of-plane bending mode frequency ν_2 (*a*'₂) for SiH₃⁺ (*X*¹*A*'₁) is 850 cm⁻¹. Pople and Curtiss²¹ give 911 cm⁻¹ for this frequency, but they note that previous experience comparing their *ab initio* frequencies and experimental values requires a scaling of the *ab initio* values by about 0.89.

The vibrational steps in Fig. 7(b) can be followed easily to ~1523 Å ≡ 8.14 eV. The region to longer wavelength has been further amplified in the inset. Here, we see a precipitous decline between 1523 and ~1531 Å, then a brief plateau before attaining the background level at ~1550 Å. In order to check the significance of the data in this region, where the signal is only ~50% larger than background, we measured the intensity at 1547.1 and 1569.5 Å (two good light intensity peaks in our H₂ lamp) five times in succession, and each time found a significant signal above background at 1547.1 Å, but not at 1569.5 Å. Therefore, we feel that the experimental result is statistically significant. Next, we examine its plausibility. There is, of course, the possibility that the SiH₃ is vibrationally hot. We cannot exclude this possibility, but our experience with other free radicals formed by abstrac-

tion reactions (NH₂, SH, SeH, OH, PH₂) has indicated that they are equilibrated at ~300 K.

At 300 K, the ratio of populations of SiH₃ in the *v*₂ (*v*' = 1) to (*v*' = 0) is 1/40–1/50. If the Franck–Condon factor for the 1→0 transition is approximated to be about the same as for the 0→1 transition, then the ratio of step heights for the first to the third step would be expected to be roughly 1/40–1/50. The observed ratio is about 1/12, providing some evidence that this first step is not a hot band.

Dyke *et al.*,¹⁴ and more recently Nimlos and Ellison,²⁴ have calculated the Franck–Condon factors, or vibrational intensity distribution in going from SiH₃ (*X*²*A*₁), pyramidal, to SiH₃⁺ (*X*¹*A*'₁), planar. Interestingly, the calculated vibrational intensity distributions look very nearly the same, but Nimlos and Ellison select 8.23 eV as the adiabatic IP, whereas Dyke *et al.* have given 8.14 ± 0.01 eV. The present limit of 1547.1 Å is equivalent to ~8.01 eV, which is approximately one vibrational quantum lower than the value of Dyke *et al.* and two lower than that of Nimlos and Ellison. If we examine the calculated Franck–Condon intensities of the first two peaks which can be measured from their respective figures, the ratio of intensities of *v*' = 1 to *v*' = 0 is about three or four to one. This is approximately the relative step height in our spectrum of the step at ~1520 Å to the step at ~1540 Å. Hence, it is plausible to expect such a weak step at onset. As explained in Sec. I, it would not have been possible for Dyke *et al.* to have extracted such a weak threshold from the spectrum available to them.

The adiabatic ionization potential of SiH₃ recently calculated by Pople and Curtiss²¹ is 7.99 eV, very close to the currently obtained value. These authors claim an accuracy of ± 0.1 eV, based upon comparison of their similarly calculated results with well-known ionization potentials.

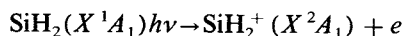
2. SiH₂

We shall begin the analysis of the photoion yield curve for this species (Fig. 8) at the highest energy, and proceed to longer wavelength. The ion yield curve for SiH₂⁺ increases sharply between 1080 and 1050 Å. We know that the fragmentation process SiH₂⁺ (SiH₄) has an onset near 1080 Å, and hence this process was suspected as the cause of the sharp rise. This was proven by turning off the microwave discharge producing F atoms. The SiH₂⁺ ion intensity in this wavelength region actually increased, because more (unreacted) SiH₄ was available for the fragmentation process. At the longer wavelengths, the SiH₂⁺ signal went to a low background level when the F atoms were not being generated.

There is a broad peak, with maximum at ~1240 Å ≡ 10.0 eV, which has some superimposed fine structure. The decline of cross section to higher energy again implies that this is an autoionizing Rydberg feature. Dyke *et al.* have calculated the vertical IP of the first excited state of SiH₂⁺ (²*B*₂) by ΔSCF to be 11.72 eV. Combining this IP with a Rydberg state at ~10.0 eV implies *n** = 2.81 for this Rydberg level, which is a plausible value. However, as shown below, their ΔSCF value for the ionization energy of the SiH₂⁺ ground state is in poor agreement with experiment,

which makes us dubious about the accuracy of their second IP, and hence of n^* . Bruna *et al.*²⁵ have calculated the relative energies of SiH₂⁺ ground and excited states, as a function of bond angle. They show the ²B₂ state preferring a very acute angle $\lesssim 30^\circ$. The excitation above the ground state is a strong function of angle. At $\sim 90^\circ$ (the neutral ground state angle) which corresponds roughly to the Franck–Condon region, the excitation of ²B₂ above X^2A_1 is about 2.8 eV, providing some support for this assignment and also for the width of the band (big angle change). The fine structure observed at the peak has spacings of about 0.23 eV, which could be vibrational structure (if the symmetric stretch is excited) or it could be evidence of more than one Rydberg series converging to the same limit.

Proceeding to longer wavelengths from the broad peak at $\sim 1240 \text{ \AA}$, we note a more or less monotonic decline to $\sim 1326 \text{ \AA}$, beyond which step structure appears. There appear to be two, or perhaps three steps (see enlarged inset), with rise points at ~ 1338 , 1354, and perhaps 1374 \AA . The 1338 and 1354 \AA rise points correspond to step widths of ~ 700 and 880 cm^{-1} , the 1374 \AA rise point to a step width of $\sim 1070 \text{ cm}^{-1}$. This step structure is suggestive of a sequence of vibrational excitations in the SiH₂⁺ (X^2A_1) ionic state. Dyke *et al.*¹⁴ calculate 966 cm^{-1} for the ν_2 bending frequency of this state, while Pople and Curtiss²¹ compute 984 cm^{-1} , with the provision that it be typically reduced by a factor of 0.89. Hence, an experimental step width $\sim 880 \text{ cm}^{-1}$ appears plausible, but the 1070 cm^{-1} width seems to be somewhat larger than would be anticipated from the calculations. The threshold for the ionization process



lies atop the process in which a metastable SiH₂ (presumably the ³B₁) is being ionized. Without knowing the shape of the ion yield curve of the metastable state between ~ 1350 – 1380 \AA , it is very difficult to know which portion of the ionization to attribute to the singlet and which to the triplet. However, it seems fairly certain that the adiabatic IP of SiH₂ (X^1A_1) is $\leq 9.15 \text{ eV} = 1355 \text{ \AA}$, and may be as low as $9.02 \text{ eV} = 1374 \text{ \AA}$. Pople and Curtiss²¹ give 9.18 eV for this adiabatic IP, whereas Dyke *et al.* give 8.49 eV by ΔSCF and 9.21 eV by Koopmans' theorem.

The weak signal from the metastable excited state can be followed fairly well to a threshold (see enlarged inset) which we have selected to be $1504 \pm 5 \text{ \AA} \equiv 8.24_4 \pm 0.025 \text{ eV}$ (see below). If we take this to be the ionization potential of SiH₂ (³B₁), and if we take the IP of SiH₂ (X^1A_1) to be 9.15 eV , then the triplet–singlet separation in SiH₂ is measured to be $0.91 \pm 0.03 \text{ eV}$.

Kasdan, Herbst, and Lineberger²⁶ obtained “an approximate upper bound to the zero-point triplet energy in SiH₂” of $\leq 0.6 \text{ eV}$ from the photodetachment spectrum of SiH₂⁻. This was said to be in agreement with Wirsam's²⁷ calculated value of 0.2 eV . Shortly thereafter, Meadows and Schaeffer²⁸ reported on a calculation at the Hartree–Fock limit for singlet–triplet separations in methylene and silylene. Some correlation was included by comparing one and two configuration results for the ¹A₁ state. Their best results (polarization functions and two configurations included)

predicted a singlet–triplet separation of 10.9 kcal/mol for CH₂ and -18.6 kcal/mol for SiH₂. After their paper had been completed and accepted for publication, they became aware of the photodetachment experimental result which placed the singlet–triplet separation of CH₂ at $19.5 \pm 0.7 \text{ kcal/mol}$. They thereupon concluded that their calculation was in error, and added to their paper an alternative calculation which yielded 19.7 kcal/mol for the methylene separation, and -10.0 kcal/mol for the silylene separation. This latter figure is cited in their abstract, and by other recent workers.²⁹

The best current evidence is that the singlet–triplet separation in CH₂ is $0.392 \pm 0.003 \text{ eV}$ ³⁰ ($9.04 \pm 0.07 \text{ kcal/mol}$), rather close to their original calculation, and our current best estimate for this separation in SiH₂ ($-0.91 \pm 0.03 \text{ eV} \equiv -21.0 \pm 0.7 \text{ kcal/mol}$) is also respectably close to their original calculation. In fact, if we interpret the adiabatic IP of SiH₂ (X^1A_1) to be as low as 9.02 eV , the singlet–triplet separation would become $0.78 \pm 0.03 \text{ eV} \equiv 18.0 \pm 0.7 \text{ kcal/mol}$.

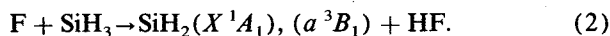
Correlation effects are evidently very important for an accurate calculation of the singlet–triplet separation. Gordon²² obtained a separation energy of 2.3 kcal/mol at the Hartree–Fock level, while Meadows and Schaeffer²⁸ obtained 5.3 kcal/mol with a single configuration for ¹A₁, but 18.6 kcal/mol with two configurations. Power *et al.*³¹ calculated 1.94 kcal/mol at the Hartree–Fock level and 10.4 kcal/mol including configuration interaction.

The interpretation of thresholds is connected with the geometry changes which may be occurring in the ionization process. For SiH₂⁺, Pople and Curtiss²¹ give a ground state (X^2A_1) structure with Si–H bond length of 1.466 \AA and an angle of 119.8° . A recent experimental result³¹ yields $r = 1.49 \pm 0.01 \text{ \AA}$ and a bond angle of $119 \pm 0.5^\circ$. For neutral SiH₂, Meadows and Schaeffer²⁸ provide 1.508 \AA and 94.3° for (X^1A_1); 1.471 \AA and 117.6° for a^3B_1 . There is very little change in angle and bond length for the ionization process $a^3B_1 \rightarrow X^2A_1 + e$, whereas there is a substantial angular change and some change in bond distance for the corresponding ionization from the ground state. For the latter case, one can expect to excite a vibrational progression in the bending mode, and perhaps also the symmetric stretch, whereas ionization of the metastable triplet state should result in a sharp Frank–Condon region, and hence a relatively steep ionization onset. This is, in fact, what is observed. Hence, we have tried to treat the threshold region of triplet ionization (at $\sim 1500 \text{ \AA}$) as being broadened primarily by rotational effects (analogous to the PH₂→PH₂⁺ study recently published.³³ The calculated shape encompasses only about 18 \AA , whereas the experimental portion appears to be broader (at least 24 \AA). Although the number of points are sparse, there appears to be an initial increase in intensity from ~ 1514 to 1504 \AA , followed by an inflection region and then an additional increase from ~ 1498 to 1486 \AA . We have chosen 1504 \AA as the rotationally adiabatic value, with an uncertainty of $\pm 5 \text{ \AA}$ which contains most of the region of increasing intensity from the background level.

By contrast, the singlet ionization process around 1350 \AA shows evidence of a vibrational progression in the bending

mode, which covers a much larger energy region.

Within the limited range of experimental conditions we attempted, it appears as if the triplet and singlet are formed in a fixed branching ratio in the reactions



Energetically, both reactions are quite exothermic, as we shall show in the next section.

Of course, the ionic intensities we observe cannot be related directly to the nascent singlet:triplet ratio, since the survival fraction of the excited triplet may be substantially smaller than the singlet, and their photoionization cross sections could also differ significantly.

We have also tried to react H atoms and O atoms with SiH₄. The calculated heats of reaction are exothermic for the production of SiH₃ and SiH₂ (*X*¹*A*₁ and *a*³*B*₁) using either H or O atoms, but about 32–34 kcal/mol less so than with F atoms. Our observation is that a given flow rate of SiH₄ which completely titrates the F atom beam reduces the H or O atom beams by $\lesssim 10\%$. Correspondingly, the SiH₃ and SiH₂ intensities are reduced by more than an order of magnitude in the H and O experiments, compared to the F experiment. Hence, although all of the relevant reactions are exothermic, the H and O atom reactions are estimated to be at least an order of magnitude slower than the F reaction, particularly for the production of SiH₃.

These conclusions are in agreement with prior kinetic studies of atomic abstraction reactions involving silane. Smith *et al.*³⁴ have shown that the F + SiH₄ reaction has a rate constant of $\sim 4.8 \times 10^{-10}$ cm³/molecule s, i.e., about six times faster than the F + CH₄ reaction. By contrast, Arthur and Bell²³ conclude from the analysis of many experiments that the H + SiH₄ reaction has a rate constant of $\sim 4.6 \times 10^{-13}$ cm³/molecule s, lower by three orders of magnitude. They also state that the "...hydrogen abstraction reactions of 'multivalent atoms' such as O ... are so insignificant as to be virtually unobservable." In our experiment, the rate of O atom and H atom reactions appeared to be comparable.

These observations concerning relative reaction rates in a sequence of abstraction reactions appear to conform to the well-established propensity rule, as enunciated by Dunning *et al.*³⁵

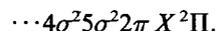
"Very exoergic reactions have small activation energies, with the activation energy increasing with decreasing exoergicity (Evans–Polanyi-type relationship)."

The H, O + SiH₄ reactions are less exoergic than the F + SiH₄ reaction by 32–34 kcal/mol. It is therefore quite likely that the barrier to reaction in the former are significantly larger than in the latter reaction. In fact, little or no barrier would be expected for the F + SiH₄ reaction, which is ~ 65 and ~ 45 kcal/mol exoergic (*vide infra*).

The ambiguity in the adiabatic ionization potential of SiH₂ (*X*¹*A*₁) could be removed if an appropriate scheme could be found which would generate this state without the concomitant production of SiH₂ (*a*³*B*₁). We are currently exploring alternative methods for formation of the desired species.

3. SiH⁺ (SiH)

The electronic configuration of SiH is



The electronic ground state *X*¹ Σ^+ of SiH⁺ results from $(2\pi)^{-1}$. No direct measure of this ionization process existed prior to the present work, but the identity mentioned in the Introduction [Eq. (1)] leads to IP (SiH) = 7.99 eV using $D_0(\text{SiH}) \leq 3.06_0$ eV given by Huber and Herzberg,¹⁶ or IP (SiH) = 8.27 ± 0.06 eV using $D_0(\text{SiH}) = 3.3414 \pm 0.0250$ eV obtained by Carlson *et al.*³⁶ The two alternative values of $D_0(\text{SiH})$ are based on observations and interpretations of two different predissociative features in the SiH spectrum. The other quantities entering into the identity, IP (Si) and $D_0(\text{SiH}^+)$, seem to be rather well established. Hence, an accurate determination of IP (SiH) could be used to distinguish between the alternative values of $D_0(\text{SiH})$.

The photoion yield spectrum of SiH⁺ seen in Fig. 9 displays a rather abrupt onset, accentuated by the presence of a sharp autoionizing feature very close to threshold. Slightly to higher energy, there is another sharp feature and then a relatively flat region, which we take to be the direct ionization. We shall choose the rotationally adiabatic value of the ionization threshold as approximately the half-rise point to the direct ionization plateau, or $1567 \text{ \AA} \equiv 7.91_2$ eV, with an error of $\pm 2 \text{ \AA} \equiv 0.01_0$ eV. We list this value, and all of the other adiabatic ionization potentials of the SiH_n free radical species obtained in this work, in Table III. Also shown are the recently calculated values of Pople and Curtiss,²¹ an earlier calculation for SiH by Rosmus and Meyer,³⁷ and the experimental value for SiH₃ of Dyke *et al.*¹⁴

Our value of IP (SiH) then leads to $D_0(\text{SiH}) = 2.98 \pm 0.03$ eV, which is probably within the error limit

TABLE III. Adiabatic ionization potentials of the SiH_n free radical species (eV).

	Present work	Pople and Curtiss ^a	Dyke <i>et al.</i> ^b	Rosmus and Meyer ^c
SiH ₃	8.01 ± 0.02	7.99	8.14 ± 0.01	
SiH ₂ (<i>X</i> ¹ <i>A</i> ₁)	9.15 ± 0.02 or 9.02 ± 0.02	8.18		
SiH ₂ (<i>a</i> ³ <i>B</i> ₁)	8.24 ± 0.02 ₅			
SiH	7.91 ± 0.01	7.81		7.93

^a Reference 21.

^b Reference 14.

^c Reference 37.

implied by Huber and Herzberg¹⁶ (upper limit 3.06₀ eV based on interpretation of Verma's³⁸ predissociation, but support also from the extrapolation³⁹ of the vibrational levels in $A^2\Delta$). The value of D_0 (SiH) preferred by Carlson *et al.*³⁶ is well outside the error range of the present study, combined with the auxiliary data. We therefore conclude that the prior interpretation of Verma's predissociation appears to be reasonable, that the criticism of this interpretation given by Carlson *et al.*³⁶ does not seem justified by the facts, and that in turn, the predissociation identified by Carlson *et al.* must be interpreted as an upper limit.

The $A^1\Pi \rightarrow X^1\Sigma^+$ emission spectrum of SiH⁺ has been studied by Douglas and Lutz,⁴⁰ and more recently by Carlson *et al.*⁴¹ From this work has come the knowledge about a strongly bound ground state ($D_0 = 3.22 \pm 0.03$ eV) and a very weakly bound $A^1\Pi$ state. The latter state can be formed from neutral SiH by



Both $^3\Pi$ and $^1\Pi$ may be expected to result from $(5\sigma)^{-1}$ ionization. Figure 10 in the chapter by Bruna *et al.*²⁵ shows the calculated juxtaposition of these states. Bruna *et al.* calculate $a^3\Pi$ to lie 2.23 eV above $X^1\Sigma^+$, with $A^1\Pi$ lying still higher. Douglas and Lutz⁴⁰ place $A^1\Pi$ at 3.102 75 eV above $X^1\Sigma^+$ (ν_{0-0}).

In Fig. 9 of the present work, one can see both broad and sharp autoionization features. These features do not appear to fit a Rydberg series converging to $A^1\Pi$. However, a plausible fit of at least the broad features can be made to a Rydberg series converging on the hitherto unobserved $a^3\Pi$ state. Our procedure was to assume the $a^3\Pi-X^1\Sigma^+$ separation given by Bruna *et al.*,²⁵ and combine it with our measured IP ($X^1\Sigma^+$) to yield a zeroth order IP ($a^3\Pi$) = 10.14 eV. The Rydberg formula was then used with this limit, and several autoionization features were tested to see if they matched a Rydberg series. With a few iterations, a rather well-behaved Rydberg series can be identified, with an improved limit at 10.21 eV. The members of this Rydberg series are indicated in Fig. 9 and included in Table IV. The inferred excitation energy $a^3\Pi-X^1\Sigma^+$ of 2.30 ± 0.01 eV is quite

TABLE IV. Autoionization features in the SiH photoionization spectrum.

Broad features matching a Rydberg series converging to $a^3\Pi$ at 10.21 eV	
λ , Å	n^*
1467	2.781
1338	3.797
1290	4.766
1265	5.768
1250	6.83
Narrow features possibly composing a Rydberg series	
1547	2.489
1363	3.495
(1299)	(4.521)
Other unidentified lines	
1560	
1440	
1406	
1347	

close to the calculated value²⁴ of 2.23 eV. The $A^1\Pi-a^3\Pi$ separation is then 0.80 eV.

The quantum defect for the broad series is indicative of d -like or possibly s -like Rydberg states, which one would expect if a p -like electron is excited. The breadth of the individual peaks, and some indication of fine structure splitting, suggests that more than one series is involved. A d -like electron combining with a $^3\Pi$ core can give rise to many states, including the states $^2\Delta$, $^2\Pi$, and $^2\Sigma$ which are optically allowed from the $^2\Pi$ ground state of SiH. In addition, a diatomic monohydride such as SiH should have a substantial rotational constant and hence the rotational fine structure could contribute to the breadth of these peaks.

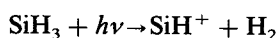
The narrow features listed in Table IV could be evidence of a p -like series, which can become allowed due to the l -spoiling of the nonspherical molecular potential.

The labeling of the individual Rydberg members in Fig. 9 in terms of principal quantum numbers is uncertain. Specifying these quantum numbers presupposes spherical symmetry, which of course does not exist. In addition, we cannot specify at this time that a particular series is predominantly s -, p -, or d -like. Hence, we have chosen to label these Rydberg members with the next higher integer to the effective quantum number.

4. SiH⁺ (SiH₃)

Under conditions where the production of SiH₃ was maximized and little SiH remained, the ion yield curve for SiH⁺ (SiH₃) shown in Fig. 10 was obtained. There is a weak onset with noticeable curvature at $\sim 1280 \pm 5$ Å $\equiv 9.68_6 \pm 0.04$ eV (see enlarged inset) and a marked increase in the slope of the ion yield curve beginning at ~ 1192 Å $\equiv 10.40$ eV.

We shall utilize the threshold for the reaction



as a test of self-consistency for the available thermochemical data. The aforementioned D_0 (SiH⁺) = 3.22 ± 0.03 eV can be used, together with $\Delta H_{f_0}^{\circ}(\text{Si}^+) = 294.63 \pm 1.0$ kcal/mol⁴² to obtain $\Delta H_{f_0}^{\circ}(\text{SiH}^+) = 272.0 \pm 1.2$ kcal/mol, very close to the value given in the JANAF table.⁴²

The threshold of Fig. 10, corrected²⁰ for the internal thermal energy of SiH₃ at 300 K, is 9.73 ± 0.04 eV = 224.4 ± 1 kcal/mol, which then gives $\Delta H_{f_0}^{\circ}(\text{SiH}_3) = 47.6 \pm 1.6$ kcal/mol. This value is in good agreement with that reported by Doncaster and Walsh,⁴³ equivalent to $\Delta H_{f_0}^{\circ}(\text{SiH}_3) = 47.7 \pm 1.2$ kcal/mol.

We have not been able to find an explanation for the increased slope beginning at ~ 1192 Å. It does not seem to be related to structure in the SiH₃⁺, no new state of SiH₃⁺ is being accessed, nor does it seem to be related to fragmentation of SiH₂.

C. Thermochemistry and bond energies

The first fragment ion from SiH₄ is SiH₂⁺, and hence its appearance potential (11.54 ± 0.01 eV), should be the most reliable. From this measurement, and using $\Delta H_{f_0}^{\circ}(\text{SiH}_4)$

$= 10.5 \pm 0.5$ kcal/mol,⁴ we can immediately determine $\Delta H_{f_0^0}(\text{SiH}_2^+) = 276.6 \pm 0.6$ kcal/mol. The next step, the determination of $\Delta H_{f_0^0}(\text{SiH}_2)$, depends upon IP (SiH₂). It will be recalled that an ambiguity existed in the interpretation of the present data, leading to IP (SiH₂) = 9.15 or 9.02 eV. The former value leads to $\Delta H_{f_0^0}(\text{SiH}_2) = 65.6$ kcal/mol, the latter value leads to $\Delta H_{f_0^0}(\text{SiH}_2) = 68.6$ kcal/mol. The corresponding values at 298 K are 0.4 kcal/mol lower. Shin and Beauchamp⁵ recently reported $\Delta H_{f_{298}^0}(\text{SiH}_2) = 69 \pm 3$ kcal/mol. The actual measurements bracketed the proton affinity of SiH₂ to be 201 ± 3 kcal/mol. To deduce $\Delta H_f(\text{SiH}_2)$, they used a value for $\Delta H_{f_0^0}(\text{SiH}_3^+) = 234.1$ kcal/mol based on Walsh's³ $\Delta H_f(\text{SiH}_3)$ and IP (SiH₃) = 8.14 ± 0.01 eV given by Dyke *et al.*¹⁴ The present study has concluded that IP (SiH₃) = 8.01 eV, which changes $\Delta H_{f_0^0}(\text{SiH}_3^+)$ to 231.1 kcal/mol and their $\Delta H_{f_0^0}(\text{SiH}_2)$ to 66 ± 3 kcal/mol. This number lies between our alternative values and hence is in somewhat better agreement with the present results. Pople *et al.* give $\Delta H_{f_0^0}(\text{SiH}_2) = 63.4$ kcal/mol, while Ho *et al.*² report 68.1 kcal/mol, a surprisingly large difference for two *ab initio* calculations of nominally the same type, which may be due to the empirical correction used by Ho *et al.*² Coincidentally, the present experimental results fitting between these values, are within the allotted errors of both calculations, i.e., ± 2 kcal/mol for Pople *et al.* and ± 3 kcal/mol anticipated by Ho *et al.*

From $\Delta H_{f_0^0}(\text{SiH}_4)$, $\Delta H_{f_0^0}(\text{SiH}_2)$, and $D_0(\text{H}_2) = 103.268$ kcal/mol⁴² we can evaluate the energy required to remove two hydrogen atoms from silane,



to be 158.4 or 161.4 kcal/mol. For comparison, the corresponding value from the *ab initio* calculations of Pople *et al.*¹ is 158.5 kcal/mol, the comparable calculation of Ho *et al.*² gives 160.9 kcal/mol and Walsh's review³ (corrected to 0 K) gives 150 kcal/mol. The heat of atomization can be calculated from $\Delta H_{f_0^0}(\text{SiH}_4)$, $D_0(\text{H}_2)$, and $\Delta H_{f_0^0}(\text{Si}) = 106.7 \pm 1$ kcal/mol⁴² to be 302.7 ± 1.1 kcal/mol. Hence, the last two bonds should sum to $144.3 + 1.2$ or 141.3 ± 1.2 kcal/mol. Again, for comparison, Pople *et al.*¹ obtain 146.0, Ho *et al.* give 141.3, and Walsh's selection yields 151.5³ kcal/mol. Hence, both our alternative data sets are in very good agreement with the *ab initio* calculations of Pople *et al.*¹ (within their target of ± 2 kcal/mol), and also with those of Ho *et al.*² and disagree by 7–8 kcal/mol with Walsh's³ values.

We can now further subdivide the bond energies. From Sec. IV A 3, $D_0(\text{SiH}) = 2.98 \pm 0.03$ eV = 68.7 ± 0.7 kcal/mol is the energy of the last bond, and hence 75.6 ± 1.4 or 72.6 ± 1.4 kcal/mol is the strength of the next-to-last bond.

For the first bond, i.e.,



we can combine our AP SiH₃⁺ (SiH₄) ≤ 12.086 eV with our

TABLE V. Heats of formation of SiH_n and SiH_n⁺, and stepwise bond energies obtained in the present study.

Heats of formation		
	$\Delta H_{f_0^0}(\text{SiH}_n)$, kcal/mol	$\Delta H_{f_0^0}(\text{SiH}_n^+)$, kcal/mol
SiH ₄	(10.5 ± 0.5) ^a	264.2 ± 0.8
SiH ₃	(47.7) ± 1.2) ^d	< 237.6 ^b
	47.6 ± 1.6	232.4 ± 1.4 ^c
SiH ₂	65.6 ± 0.7 or 68.6 ± 0.8 ^c	276.6 ± 0.6
SiH	89.6 ± 1.2	272.0 ± 1.2
Step-wise bond energies ΔH_0 , kcal/mol		
SiH ₄ → SiH ₃ + H	88.8 ± 1.6	
SiH ₃ → SiH ₂ + H	69.6 ± 2.1 or 72.5 ± 2.1 ^c	
SiH ₂ → SiH + H	72.6 ± 1.4 or 75.6 ± 1.4 ^c	
SiH → Si + H	68.7 ± 0.7	

^a From Ref. 4; Most of the values presented in the table above are based on this reference value for $\Delta H_f^0(\text{SiH}_4)$.

^b From the threshold of SiH₃⁺ (SiH₄).

^c From $\Delta H_f^0(\text{SiH}_3)$ of Ref. 43 and the presently obtained IP (SiH₃).

^d From Ref. 43.

^e Alternative values are based on the two possible values of the adiabatic IP of SiH₂ (¹A₁).

IP (SiH₃) = 8.01 eV to obtain ≤ 4.076 eV $\equiv 94.0$ kcal/mol. The fact that AP (SiH₃⁺) is a second threshold, together with its pronounced curvature, leads us to the view that this measurement is just a limit, and that the true value of this bond is smaller. Walsh³ gives 88.3 kcal/mol (0 K), Ho *et al.*² obtain 90.1 kcal/mol, and Pople *et al.*¹ report 91.7 kcal/mol.

If we adopt $\Delta H_{f_{298}^0}(\text{SiH}_3) = 46.4 \pm 1.2$ kcal/mol from Doncaster and Walsh,⁴³ our alternative values for $\Delta H_{f_0^0}(\text{SiH}_2)$ lead to 69.5 ± 1.4 or 72.5 ± 1.4 kcal/mol for the reaction



These stepwise bond energies, and the related heats of formation, are summarized in Table V.

Although there is no obvious experimental basis for choosing between IP (SiH₂ X¹A₁) = 9.15 ± 0.02 and 9.02 ± 0.02 eV, it may be significant that the 9.15 eV value is not only in better agreement with the calculated IP = 9.18 eV obtained by Pople and Curtiss,²¹ but using this ionization potential also yields the bond energies $D_0(\text{HSi-H}) = 75.6 \pm 1.4$ kcal/mol and $D_0(\text{H}_2\text{Si-H}) = 69.6 \pm 2.1$ kcal/mol, which are in good agreement with the calculated values of Refs. 1, 21, and 2, and in fact fall between their numbers.

Finally, we note that the reaction of F atoms with SiH₃ to produce SiH₂ + HF is exothermic by 62.6 or 65.6 kcal/mol if SiH₂ is formed in the X¹A₁ state, and still exothermic by 44.6 ± 0.8 kcal/mol if formed in the a³B₁ state. In these calculations, $\Delta H_{f_0^0}(\text{HF})$ and $\Delta H_{f_0^0}(\text{F})$ are taken from Ref. 42.

This research was supported by the U.S. Department of Energy, Office of Basic Energy Sciences, under Contract No.

W-31-109-Eng-38, and by the U.S. Yugoslav Joint Board for Science and Technology through the U.S. Department of Energy Grant JFP 561.

- ¹J. A. Pople, B. T. Luke, M. J. Frisch, and J. S. Binkley, *J. Phys. Chem.* **89**, 2198 (1985).
- ²P. Ho, M. E. Coltrin, J. S. Binkley, and C. F. Melius, *J. Phys. Chem.* **89**, 4647 (1985).
- ³R. Walsh, *Acc. Chem. Res.* **14**, 246 (1981).
- ⁴S. R. Gunn and L. H. Green, *J. Phys. Chem.* **65**, 779 (1961).
- ⁵S. K. Shin and J. L. Beauchamp, *J. Phys. Chem.* **90**, 1507 (1986).
- ⁶A. W. Potts and W. C. Price, *Proc. R. Soc. London Ser. A* **326**, 165 (1972).
- ⁷B. P. Pullen, T. A. Carlson, W. E. Moddeman, G. K. Schweitzer, W. E. Bull, and F. A. Grimm, *J. Chem. Phys.* **53**, 768 (1970).
- ⁸R. R. Corderman and J. L. Beauchamp, unpublished but quoted by Ref. 14.
- ⁹A. Ding, R. A. Cassidy, L. S. Cordis, and F. W. Lampe, *J. Chem. Phys.* **83**, 3426 (1985).
- ¹⁰K. Börnin, T. Heinis, and M. Jungen, *Chem. Phys.* **103**, 93 (1986).
- ¹¹See, for example, J. Berkowitz, *Photoabsorption, Photoionization and Photoelectron Spectroscopy* (Academic, New York, 1979), pp. 274–280.
- ¹²J. D. Morrison and J. C. Traeger, *Int. J. Mass Spectrom. Ion Phys.* **11**, 289 (1973).
- ¹³W. Genuit, A. J. H. Boerboom, and T. R. Gover, *Int. J. Mass Spectrom. Ion Process.* **62**, 341 (1984).
- ¹⁴J. M. Dyke, N. Jonathan, A. Morris, A. Ridha, and M. J. Winter, *Chem. Phys.* **81**, 481 (1983).
- ¹⁵C. M. Brown, *J. Opt. Soc. Am.* **64**, 1665 (1974).
- ¹⁶K. P. Huber and G. Herzberg, *Molecular Spectra and Molecular Structure. IV. Constants of Diatomic Molecules* (Van Nostrand Reinhold, New York, 1979).
- ¹⁷J. L. Elkind and P. B. Armentrout, *J. Phys. Chem.* **88**, 5454 (1984) obtain $D_0(\text{SiH}^+) = 3.23 \pm 0.04$ eV, and cite earlier spectroscopic studies which yield $D_0(\text{SiH}^+) = 3.22 \pm 0.03$ eV.
- ¹⁸S. T. Gibson, J. P. Greene, and J. Berkowitz, *J. Chem. Phys.* **83**, 4319 (1985).
- ¹⁹T. Heinis, K. Börnin, and M. Jungen, *Chem. Phys. Lett.* **110**, 429 (1984).
- ²⁰P. M. Guyon and J. Berkowitz, *J. Chem. Phys.* **54**, 1814 (1971).
- ²¹J. A. Pople and L. A. Curtiss, *J. Phys. Chem.* (submitted).
- ²²M. Gordon, *Chem. Phys. Lett.* **59**, 410 (1978).
- ²³N. L. Arthur and T. N. Bell, *Rev. Chem. Intermediates* **2**, 37 (1978).
- ²⁴M. R. Nimlos and G. B. Ellison, *J. Am. Chem. Soc.* **108**, 6522 (1986).
- ²⁵P. J. Bruna, G. Hirsch, R. J. Buenker, and S. D. Peyerimhoff, in *Molecular Ions—Geometric and Electron Structures*, edited by J. Berkowitz and K.-O. Groeneveld (Plenum, New York, 1983), p. 323.
- ²⁶A. Kasdan, E. Herbst, and W. C. Lineberger, *J. Chem. Phys.* **62**, 541 (1975).
- ²⁷B. Wirsam, *Chem. Phys. Lett.* **14**, 214 (1972).
- ²⁸J. H. Meadows and H. F. Schaeffer, III, *J. Am. Chem. Soc.* **98**, 4383 (1976).
- ²⁹G. Inouye and M. Suzuki, *Chem. Phys. Lett.* **122**, 361 (1985).
- ³⁰A. R. W. McKellar, P. R. Bunker, T. J. Sears, K. M. Evenson, R. J. Saykally, and S. R. Langhoff, *J. Chem. Phys.* **79**, 5251 (1983).
- ³¹D. Power, P. Brint, and T. Spalding, *J. Mol. Struct.* **108**, 81 (1984).
- ³²M. C. Curtis, P. A. Jackson, P. J. Sarre, and C. J. Whitham, *Mol. Phys.* **56**, 485 (1985).
- ³³J. Berkowitz, L. A. Curtiss, S. T. Gibson, J. P. Greene, G. L. Hillhouse, and J. A. Pople, *J. Chem. Phys.* **84**, 375 (1986).
- ³⁴D. J. Smith, D. W. Setser, K. C. Kim, and D. J. Bogan, *J. Phys. Chem.* **81**, 898 (1977).
- ³⁵T. H. Dunning, Jr., L. B. Harding, R. A. Bair, R. A. Eades, and R. L. Shepard, *J. Phys. Chem.* **90**, 344 (1986).
- ³⁶T. A. Carlson, N. Durić, P. Erman, and M. Larsson, *J. Phys. B* **11**, 3667 (1978).
- ³⁷P. Rosmus and W. Meyer, *J. Chem. Phys.* **66**, 13 (1977).
- ³⁸R. D. Verma, *Can. J. Phys.* **43**, 2136 (1965).
- ³⁹A. E. Douglas, *Can. J. Phys.* **35**, 71 (1957).
- ⁴⁰A. E. Douglas and B. L. Lutz, *Can. J. Phys.* **48**, 247 (1970).
- ⁴¹T. A. Carlson, J. Copley, N. Durić, N. Elander, P. Erman, M. Larsson, and M. Lyyra, *Astron. Astrophys.* **83**, 238 (1980).
- ⁴²M. W. Chase, J. L. Curnutt, J. R. Downey, R. A. McDonald, A. N. Syverud, and E. A. Valenzuela, *J. Phys. Chem. Ref. Data* **11**, 695 (1982).
- ⁴³A. M. Doncaster and R. Walsh, *Int. J. Chem. Kinet.* **13**, 503 (1981).